Residual Stress Measurement on T-type Welded Specimen by Neutron Diffraction

D. Y. Jang, M. J. Park, H. D. Choi and J. P. Kim

Abstract

This paper presents application of neutron diffraction technique to the measurement of residual stresses in the T-type 20 mm thick welded stainless steel plates(100×50 mm^2 and 50×50 mm^2). The High Resolution Powder Diffractormeter of the Korea Atomic Research Institute was utilized in the measurement. The power of nuclear reactor was 24 MWt and the measured reflection in the 220 plane (2θ) was 92.66°. Poisson ratio of 0.265 and elastic constant of 211 GPa were applied to the calculation of stresses and strains. Three directional components such as normal, transverse, and longitudinal stresses were measured. The results showed that three components were tensile and became compressive along the y axis in the zone away from the welded center. The compressive stresses became tensile in the zone away from the center line of x axis. This may be due to the balance effect caused by the net stress to keep the specimen shape flat.

1. Introduction

Welding residual stress is thermal stress (primary cooling stress) with possibly superimposed transformation stress[1]. The thermal stress is caused by the thermal expansion proportional to the temperature changes. The transformation stress is caused by transformation strain which occurs in ferritic steel as a result of the $\gamma - \alpha$ transformation. The nature and scope of this transformation depends on the cooling rate, austenite retention time, and austenite peak temperature. This complex metallurgical process in welding, such as shrinkage, quenching, or phase transformation, produces both tensile or compressive residual stress in different zones of the welded structure.

Residual stress, particularly tensile residual stress in the weldment, can be a very important factor to affect the reliability and integrity of the weld. The formation of tensile residual stress may result in initiation of fatigue cracks, stress corrosion cracking, or other types of fracture. Tensile stresses in the welded zone limit the fatigue resistance of the component under cyclic loading. In an aggressive environment, tensile welding residual stresses also create a necessary condition for stress corrosion cracking to take place. It is important, therefore, to understand the distribution of residual stress in and near the weldment.

Residual stress states are of two types: macrostress and microstress[2]. Macrostresses are those residual stresses which are in equilibrium within macrodomains, covering volumes comparable in size to the part; they concur with the concept of isotropic material. Macrostresses are the most commonly studied as they can affect the service performance of a component.

Microstresses are crystal stresses within single metal grains or groups of grains in equilibrium within volumes comparable with dimensions of the grains. These include submicroscopic stresses which are relate to distortions in atomic lattices of crystals. They tend to occur in multiphase alloys and composites due to differences in thermal expansion coefficients between phases.

Residual stresses may be determined by either analytical or experimental methods[2,3]. Analytical methods, developed by a number of authors using finite element methods, allow us to compute the distribution of residual stresses in the surface layer on the basis of the following factors: mechanical properties of the processed material, shape and dimensions of the part, and the loading condition. Because of the complexity of these methods, their application is limited. Often, important data is unavailable, such as strength and heat sources. Or, the predicted residual stresses are inaccurate. In view of the above, the residual stresses are determined mostly by experimental methods[2,3]. The experimental methods are divided into destructive and nondestructive methods.

In the destructive methods, the residual stresses are derived from measurements of deformations occurring after cutting the inspected part. The methods are based on the assumption that cutting the part along a given

D.Y. Jang and ***J. P. Kim*** are an Associate Professor and an Assistant Professor of Industrial Information Systems Enginering Department, Seoul National University of Technology, Seoul, Korea
M. J. Park is a Ph.D Student of Seoul National University
H. D. Choi is an Associate Professor, Seoul National University
E-mail : dyjang@duck.snut.ac.kr TEL : +82-2-970-6450

section is equivalent to applying stresses to the cut surface that are opposite to the residual stresses. These opposite stresses either cause deformations in the part or reaction forces in holding devices. By measuring the deformations or reaction forces the magnitude of residual stresses is derived. The destructive methods may be subdivided further into those that completely destroy the inspected part and those causing a partial destruction only. (Almost all destructive methods in use today involve complete destruction).

Nondestructive experimental methods[2,3,4] are based on measurements of electromagnetic, optic and other physical phenomena in the residual stress field. Residual stresses are measured in the tangential, axial and radial directions. Of all the residual stress measuring techniques, diffraction methods are widely accepted as the most general and reliable nondestructive method of quantifying the residual stress tensor. Diffraction methods use the atomic planes of the crystalline grains within the material as very sensitive strain sensors. Analysis techniques permit separation of long range macrostresses and short range or grain-to-grain microstresses.

There have been several experimental and computational studies of welded austenitic steel plates by neutron diffraction[3,5]. Single-pass and multi-pass weldments were measured by using neutron diffraction and residual stress distributions as well as stain were mapped out in the heat affected zone of the weldments. T-type welded joints are usually obtained by fillet welding with edge preparation and generally applied to construction of big structures. Their safety and reliability are critical to the safe operation and usage of the structures. Hence, information of residual stress distribution on the T-type welded joint is important and could be obtained through accurate measurements. Because of its relatively large size of the T-type welded joint, it is better to use neutron diffraction. No study of residual stress measurement on the T-type welded joint by neutron diffraction has been reported. In this research, the austenitic stainless steel sample with T fillet welded joint was designed to simulate the joint of structure and residual stress distributions along the fusion line and, in and near the heat affected zone of the weldment were measured. The neutron diffractometer of the Korean Atomic Energy Research Institute was utilized to map three orthogonal components of residual stress at selected locations within the weldment. This research could provide a way to utilize the neutron diffraction technique in the fatigue design of large structures and machine elements, and to improve reliability and fatigue life of machinery.

2. Theory of diffraction technique

Diffraction is the principal non-destructive means of measuring residual stresses. Two main ideas are involved. First, if a residual stress (strain) is present in a sample, the interplanar spacings are altered relative to the unstressed state, causing shifts in the position of diffraction peaks. Second, under a given stress, the peak position generally changes with sample orientation. Because engineering materials are polycrystalline, there will be grains oriented to diffract in any sample orientation for a given peak. Residual stress state are measured by systematically changing the sample orientation, observing the shifts in peak position, then converting the shifts first to strains, then to stresses, using elasticity theory.

In x-ray and neutron diffraction, polycrystalline solid or powdered specimens are placed in a monoenergetic, collimated beam. Appropriately oriented grains diffract the x-rays or neutrons into a detector. By sweeping the angles of incidence and detection, a spectrum of diffraction peaks corresponding to the crystal lattice spacings is produced. The measured lattice spacings are compared with spacings of known compounds to identify the crystalline phases and are used to define the unit cell parameters. Analysis of unit cell parameters as a function of temperature yields the lattice thermal expansion. Reactions, phase transformation, and crystallization are all studied by high temperature diffraction methods. Crystal structure analysis (e.g. atomic location, thermal motion, site occupancy) utilizes both the line position and intensity[6].

Neutrons penetrate many millimeters to centimeters in most engineering materials; thus, through thickness, macro residual strain measurements are possible. This may be seen through a comparison of values of the depth below the surface from which 50% of the diffracted beam originates for neutrons vs. X-rays[2].

It should be noted that with diffraction, only the elastic component of the strain tensor is measured; any plastic strains are not determinable via diffraction. Strains measured with diffraction are also along a particular crystallographic direction that has its own elastic constants that will, in general, differ from the bulk values and will vary with preferred orientation. Since stress is a tensor, measurements are required in six orientations to completely determine the stress state at a point. However, when the principle directions are known, three orientations are sufficient. Neutron diffraction measurements use lattice-spacing as a strain gauge. They are obtained from Bragg's law[2].

$$n \cdot \lambda = 2d \cdot \sin\theta \quad (1)$$

where n is an integer, λ is the wavelength of the radiation, d is the lattice-spacing, and θ is the diffraction angle corresponding to a particular hkl reflecting plane. Strain is measured in the direction of the scattering vector Q that bisects the incident and diffracted beams. In order to satisfy equation (1), any change in lattice spacing $\Delta d = d - d_0$, where d_0 is the unstrained lattice spacing, will result in a change in or and strain is given by

$$\varepsilon = \frac{d - d_0}{d_0} \tag{2}$$

For the welding sample, because of symmetry the principal directions coincide, with the normal, transverse and radial directions, so that measurements of strain in these orientations only are needed to completely define the stress tensor at a point. In order to obtain adequate resolution a suitable small 'gauge volume', as Fig. 1 in which the measurements are made, must be defined.

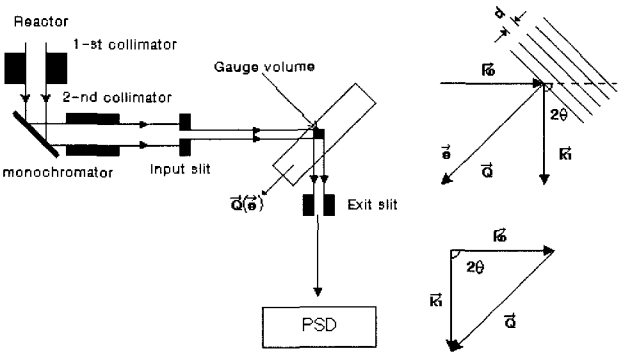

Fig.1 Strain measurement schematic

To make measurements it is necessary to precisely position and align the sample to be examined in the diffractometer. The spatial resolution of a neutron measurement depends on the dimensions of the apertures masking the beam as well as on the angle between the incident and diffracted beams. When the principal directions coincide with the coordinate directions normal, transverse and axial and the material is isotropic with a Young's modulus E and Poisson's ration ν, the principal stresses are obtained from

$$\begin{aligned}
&\text{– Normal direction : } \sigma_{11} = \frac{E}{(1+\nu)}\left[\varepsilon_{11} + \frac{\nu}{1-2\nu}(\varepsilon_{11}+\varepsilon_{22}+\varepsilon_{33})\right] \\
&\text{– Transverse direction :} \\
&\sigma_{22} = \frac{E}{(1+\nu)}\left[\varepsilon_{22} + \frac{\nu}{1-2\nu}(\varepsilon_{11}+\varepsilon_{22}+\varepsilon_{33})\right] \\
&\text{– Axial direction : } \sigma_{33} = \frac{E}{(1+\nu)}\left[\varepsilon_{33} + \frac{\nu}{1-2\nu}(\varepsilon_{11}+\varepsilon_{22}+\varepsilon_{33})\right]
\end{aligned} \tag{3}$$

3. Experiments

The sample was prepared by using two SUS304 stainless steel plates of size $100\times50\times20$ mm^3 and $50\times50\times20$ mm^3. As shown in Fig. 2 and Fig. 3, two plates with chamfers at the two edges of the one side of the plate were welded by multipass Tic-arc welding at current 130-140 A and voltage 25-27 V, resulting in T fillet joint. The Cartesian coordinate system was adopted for the strain components as shown in Fig. 3 The principal strain directions are defined by normal (y axis), transverse (x axis), and longitudinal (axial or z axis) directions. Each component of strain is measured by aligning the specimen position with the scattered vector Q. Fig. 4 shows the measurement procedure where the accurate position and movement of the welded specimen are critical to the precise measurement. In the neutron diffraction, the spatial resolution of the beam depends on the size of the beam slit and angles between the incident and scattered beams. Two 2 mm wide slits of beam in absorbing cadmium sheets were placed in the incident and scattered beams to define the gauge volume over which the strain is measured as shown in Fig. 1. For the normal and transverse components with relatively low strain gradient, height of the incident slit was 24mm and width of it was 2mm in the measurement. In order to measure longitudinal strain with high strain gradient, beam of 4mm height and 2mm width was utilized. The strain profile in the welded specimen was measured by moving the specimen gradually.

Neutron diffraction experiments were carried out on the High Resolution Powder Diffractometer (HRPD) that is put into operations at the 24 MWt HANARO reactor in Korea Atomic Energy Research Institute(KAERI). The 220 reflection was selected since the diffraction elastic constants are close to the bulk values and the assessment of residual stress is simplified. The incident neutron beam is made monochromatic by diffraction from the 220 plane of a welding sample. The SUS 304 steel, on the (220) plane gives a scattering angle 2θ of 92.66°. Narrow incident and receiving slits define the gauge volume within the specimen as shown in Fig. 1. The neutrons are counted in a position sensitive detector (PSD). The free-stressed lattice distance d_0 is measured by the neutron diffraction using the sample that is obtained by cutting the small corner part of the welded specimen. The measured d_0 is used as the reference value of d in the measurements. The diffraction peak 220 ($\theta_{220} \fallingdotseq 92.66°$) is scanned. The peak centers, widths and intensities are obtained by least squares fittings a Gaussian line shape to the experimental data. Fig. 5 shows positions of the measured specimen according to its measuring direction. Since it is necessary to change the measuring direction according to the distance of beam path, the normal component is measured by reversing the measuring direction, differently from the other two directions. Since it is not easy to decide the

beam path on the T fillet welded specimen, the measurement time is different according to the measuring points. The sample is assumed to be symmetry with respect to y axis. The typical error in strain was 30×10^{-6}. Normal strain component along the normal direction is measured with 2.5mm step in the region between 0mm and 30mm position in x direction and between 0mm and 30mm in y direction. The transverse stress component was also measured in the similar way to measurement of normal component by fixing the specimen to the direction of Q vector. The longitudinal component was measured in the region of $0 \leq x \leq 30$ mm, and $0 \leq y \leq 30$ mm. Stresses were calculated using effective elastic diffraction constants E = 211 GPa and ν = 0.265 for 304L stainless steel for reflection 220.

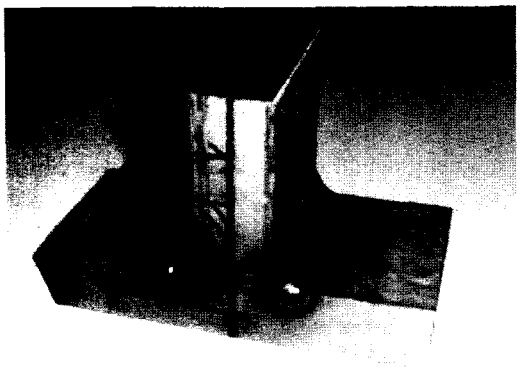

Fig.2 Measured welding sample

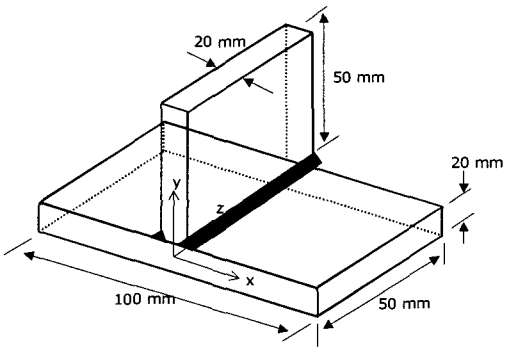

Fig.3 Measured welding sample coordinate system

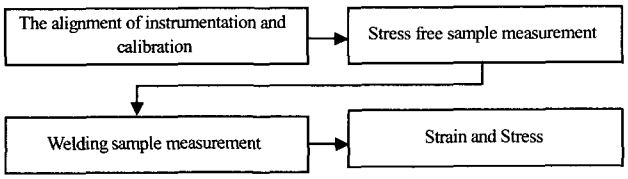

Fig.4 Measurement procedures

Table 1 Chemical composition (%)

C	Si	Mn	P	S	Ni	Cr
0.08	1.00	2.00	0.040	0.03	8~10.5	18~20

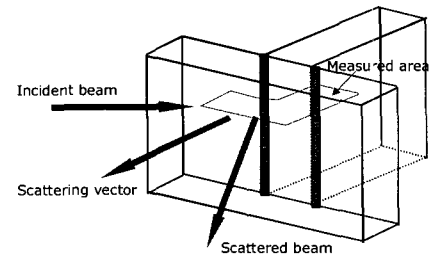

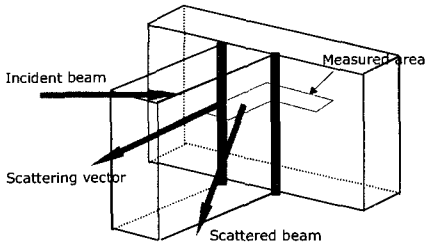

(a) Normal direction

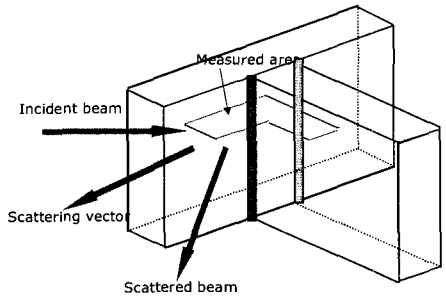

(b) Transverse direction

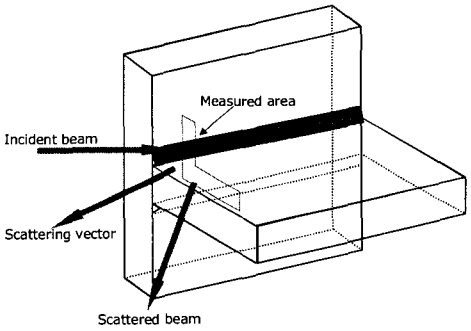

(c) Longitudinal(axial) direction

Fig.5 Measurement of each direction component

The nominal chemical composition and mechanical properties of the specimen are given in Table 1.

Table 2 Mechanical properties

Tensile Strength (MPa)	Yield Strength (MPa)	Elongation (%)
> 505	> 480	> 40

4. Results and discussion

The variation of residual stresses of the three principal directions, normal, longitudinal, and transverse stresses, is shown in Fig. 6. These stresses were obtained by applying measured residual strains to equation (2) and (3). The normal stress at y = 0 and x = 0 (center point) was compressive although the other components (transverse and axial stresses) were compressive. The normal stress (surface) at y = 0 was changed to tensile and then close to zero as the measurement positions were away from the center. This stress could be considered negligible. Transverse and axial stresses were tensile. Three stresses at y = 5 and 7.5 mm showed similar trend along the x axis. In the fillet area around y = 12.5 mm and x = 12.5 mm, the transverse stress was tensile or close to zero but the normal stress and axial stress were compressive. This effect showed that transverse direction didn't receive much effect by the welding and the stress profile could be considered as the plane stress condition in terms of normal and axial components. Three directional stresses at the height of y ≤ 12.5 mm showed similar trend of variation. They were tensile at the area close to the weld center and then changed to high compressive, returning to tensile again in the zone away from the welding center. The transverse stress became tensile close to the surface in the area close to the center of weldment. The other components also showed similar results, tensile at on the surface of the weldment and compressive in the inner part of the weldment. This may be caused by the welding geometry of this sample. Since the T type fillet welding may generate net effect of the stress to balance the geometry and keep the top and bottom surfaces of this sample flat. This may balance out the shrinkage of the specimen.

The physical phenomena that cause residual stresses, such as thermal gradients and plastic yield, are often directional and coupled to stresses in parallel directions. There could be three possible physical phenomena that contribute to the final stress state of the welded plate. First, shrinkage effect is caused by the weld metal solidification on the top of a solid substrate such as base metal or previously deposited weld layers. The resultant stresses are generated parallel to the line of the weld. It is the longest dimension for shrinkage. Shrinkage effects also exist in the direction perpendicular to the long dimension of the weld since the core of the weld will solidify and contract slowly that the surface, resulting in triaxial tension in the fusion zone. Second, temperature gradients between outside and inside of the plate can generate thermal stresses that vary through the thickness. Third, the phase transformation from austenite to martensite is associated with volume change during cooling from high temperature. These three mechanisms could be the sources to the residual stresses. The longitudinal shrinkage of the fusion zone may be the main source of the longitudinal components of stress. The fusion zone and heat affected zone are constrained by the unyielded portions of the base metal plate, resulting in a state of residual tension and base plate left in compression. Closer to the fusion zone, other geometric effects and yielding mechanism could create more complex residual stress patterns.

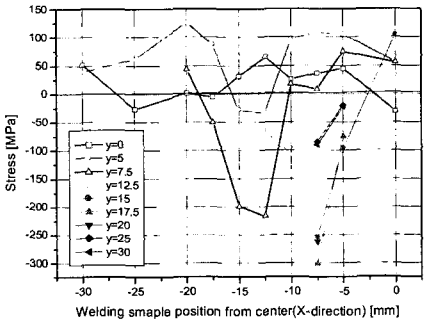

(a) Stress distribution(normal direction)

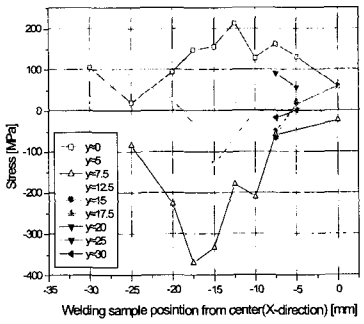

(b) Stress distribution(transverse)

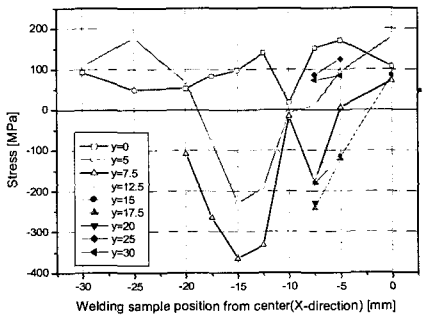

(c) Stress distribution(axial direction)

Fig.6 The stress distribution in welded SUS304 plate

Since the structural change causes the residual stress generation, it may scatter the neutron beam on the lattice plane. This scattering rate or diffraction rate of neutron can be measured by the attenuated neutron strength on the lattice plane. Fig. 7 shows neutron peak area for stainless sample according to the path length in the stainless steel sample. By using two stressed and unstressed specimens, the measured neutron peak areas according to the path length of neutron were calculated. The neutron attenuation index is 1.116cm^{-1} for unwelded specimen and show concentrated data along the fitted line. However, the stressed domain by welding shows scattering of data.

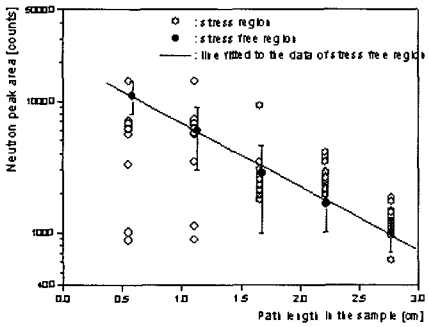

Fig.7 Measured neutron peak area for the stainless steel sample according to the path length in the sample

5. Conclusion

The residual stress distributions on the T-type welding specimen were measured by using neutron diffraction in the research. Stresses were tensile at the area close to the welded center and then changed to high compressive, returning to tensile again in the zone away from the center of welded workpiece. The transverse stress became tensile in region close to the surface in the weld center zone. The normal and longitudinal stresses also showed similar results, tensile at on the surface of the weldment and compressive in the inner part of the weldment. This might be caused by the welding geometry of this sample and T fillet welding may generate net effect of the stress to balance the geometry and keep the top and bottom surfaces of this sample flat.

Another important conclusion was that the neutron diffraction provided us a way to understand the residual stress fields created by the welding and the large scale features of the spatial distribution of residual stresses in the large structures could be measured. This research could provide a way to utilize the neutron diffraction technique in the fatigue design of large structures and machine elements and to improve reliability and fatigue life of machinery.

Acknowledgements

The authors wish to thank the reviewers for their helpful comments on the paper. This research could be completed due to the financial support form Seoul National University of Technology through the Faculty Development Fund. The authors also thank Korea Ministry of Science and Technology for its support.

References

1. K. Masubuchi: Analysis of Welded Structures, *Pergamon Press*, (1980)
2. A. D. Krawitz: Residual Stress Analysis with Neutrons, *Mat. Res. Soc. Symp. Proc.*, Vol. 166 (1987), pp.281-292
3. M. J. Park, D. Y. Jang, and H. D. Choi: Residual Stress Measurement on Welded Stainless Steel Specimen by Neutron Diffraction, *Int. J. Korea Welding Society*, Vol. 1 (2001), pp.39-43
4. S. P. Prey: X-ray Diffraction Residual Stress Techniques, *Metal Handbook, 10, Metals, OH: American Society for Metals*, (1986), pp.380-392
5. J. H. Root, T. M. Holden, J. Schroder, C. R. Hubbard, S. Spooner, T. A. Dodson and S. A. David: Residual Stress Mapping in Multipass Ferritic Steel Weld, *Material Science and Technology*, Vol. 9 (1993), pp.754-759
6. I. C. Noyan and J. B. Cohen: Residual Stress Measurement by Diffraction and Interpretation, *Springer-Verlag, New York*, (1987)